Journal Pre-proof

New technique for determining the critical freezing temperatures of chicken breast based on radiofrequency photospectrometry

Juan Angel Tomas-Egea, Marta Castro-Giraldez, Ricardo J. Colom, Pedro J. Fito

PII: S0260-8774(22)00209-6

DOI: https://doi.org/10.1016/j.jfoodeng.2022.111155

Reference: JFOE 111155

To appear in: *Journal of Food Engineering*

Received Date: 10 December 2021

Revised Date: 4 May 2022

Accepted Date: 26 May 2022

CRediT authorship contribution statement

Juan Angel Tomas-Egea: experimental research, conceptualization, methodology, validation, investigation, resources– original draft. **Marta Castro-Giraldez**: conceptualization, methodology, sensor design, validation, formal analysis, investigation, resources, writing – original draft, supervision, project administration and funding acquisition. **Ricardo J. Colom**: conceptualization, methodology, sensor design, resources– original draft, project administration and funding acquisition. **Pedro J. Fito**: conceptualization, methodology, sensor design, validation, formal analysis, investigation, resources, writing – original draft, supervision, project administration and funding acquisition.

NEW TECHNIQUE FOR DETERMINING THE CRITICAL FREEZING TEMPERATURES OF CHICKEN BREAST BASED ON RADIOFREQUENCY PHOTOSPECTROMETRY

Juan Angel Tomas-Egea[1], Marta Castro-Giraldez[1*], Ricardo J. Colom[2] and Pedro J. Fito[1]

[1] Instituto Universitario de Ingeniería de Alimentos para el Desarrollo, Universitat Politècnica de València, Camino de Vera s/n, 46022 Valencia, Spain.

[2] Instituto de Instrumentación para Imagen Molecular, Universitat Politècnica de Valencia, Camino de Vera s/n, 46022 Valencia, Spain

* marcasgi@upv.es

Abstract

Food freezing operations require an extreme knowledge of the thermal properties of the food to be frozen, in order to achieve a product that at the thawing time preserves the best sensory and food quality properties, and also preserves food safety. Within these properties it is necessary to know the initial freezing temperature (T_{m0}), the freezing temperature of the maximally freeze concentrated liquid phase (T_m'), the glass-transition temperature of the maximally freeze concentrated liquid phase (T_g') and others. However, the techniques to determine these properties are long, tedious, and sometimes with high variability, one of the most important technique is Differential Scanning Calorimetry (DSC). In this work, the use of photospectrometry in the radiofrequency range (PFR) is proposed, as a fast and reliable method for determining the thermal properties of chicken breast in the freezing process, comparing it with the DSC technique. The results showed a Tg' of -17.50 ± 1.05, obtained by the PFR technique, using the beta dispersion, similar as the result obtained by DSC technique (-16.73 °C ± 0.13). Therefore, the PFR is a fast, reliable, and easy technique to determine the critical temperatures of the food freezing process.

Keywords: Permittivity, glass transition, chicken freezing, dielectric properties

1. Introduction

The food freezing operation, as well as the freezing of any biological system, has been studied for a long time due to its high preservation capacity, remaining good quality and safety parameters (Kumar et al., 2020; van der Sman, 2020). The mathematical models developed to predict the stability of frozen food are based on the knowledge of physical and chemical properties that determine the different behaviors induced, in raw matter tissue, during the freezing process. Some of these properties are: the medium capacity to store or transmit heat, the state variables variation to produce the water freezing (and other compounds with change state capacity), the medium glass transition and the nature of solutes with cryoprotective capacity to minimize the internal breakage (Elliott et al., 2017).

Freezing theory explains that the ice nucleation (formation of the incipient crystalline phase), in biological systems, is produced in supercooling and heterogeneous liquid phase, with thermal fluctuations produced by the exothermic transition (You et al., 2021), followed by ice clusters formation or ice crystals growth induced by ice surface tension and water phase transition (Castro-Giraldez et al., 2014). When freezing operation is produced slowly, at the melting temperature (Tm'), the amount of ice formed is maximum and the remaining liquid phase is called the maximally freeze concentrated solution. If temperature continues decreasing, the system reaches the glass transition temperature (Tg') and the maximally freeze concentrated solution increases dramatically its viscosity and becomes a supercooling liquid glass. Foods below glass transition temperature show maximum stability. This is why it is important to know the critical temperatures of the food freezing process, initial freezing temperature (Tm_0), the freezing temperature of sample with the maximally freeze-concentrated solute matrix (Tm') or the glass transition temperature of the maximally freeze-concentrated solute matrix (Tg') (Roos, 2021), which means the product has reached its lowest water activity (a_w^c) (Roudaut et al., 2004).

The changes in the state of the unfrozen phase during the freezing operation are shown in the food diagram State (Van der Sman, 2020), where freezing line and glass transition curve are limited by the critical temperatures exposed before. Freezing line was modelled by Robinson and Stokes (2002), Chirife and Fontan (1980) or Chen (1986). The prediction of the water activity and the initial freezing point from composition of meat products was modelled by van der Sman and Boer (2005). A model based on thermodynamics to study the driving forces and to explain the nucleation of water was reported by Hellmuth et al. (2020). Glass transition line was modeled by Gordon and Taylor (1952), being the most widely used model to describe this transformation.

Photospectrometry in different ranges of the electromagnetic spectrum has been used to determine different properties of water in food. At low energy range, radiofrequency and microwave ranges, the interaction with matter can be modeled by Schrodinger's equation (Roychoudhuri et al,, 2008) attending to the quantum theory. However, at the macroscopic level, it is possible to apply the Maxwell's equations (Horie et al., 2000) where the physical property that describes the electric effect is the complex permittivity and for the magnetic effect is the complex permeability (Baker-Jarvis et al., 2012).

In the radiofrequency range, the main effect is electrical, having three molecular interactions of photons: The alpha dispersion or counterion effect (in the Hz-kHz range), where photons induce an orientation to electrolytes with high ionic strength. The beta dispersion or Maxwell-Wagner effect (in the MHz range), where fixed charges from macromolecules or charges generated by surface tension are oriented (Traffano-Schiffo, et al., 2018). Finally, the ionic conductivity (in the Hz-1 GHz range), a phenomenon that only generates electrical losses due to the vibration of low molecular weight electrolytes with high ionic strength. Some authors relate the variation of permittivity in alpha and beta dispersions with the glass transition (Mahanta et al., 2017; Roos, 2020).

The aim of this work is to develop a new technique to determine the critical freezing and glass temperatures of chicken breast using the photospectrometry in the radiofrequency range technique (PRF).

2. Materials and methods

2.1. Experimental procedure

Each experiment was carried out using two cylinders of 2 cm in diameter and 2 cm in height, obtained from boneless chicken breasts at “Productos Florida” slaughterhouse, located in Almazora, Castellón, Spain, with 36 hours postmortem. The cylinders were obtained perpendicular to the fibres using a 2 cm diameter coreborer. One of the cylinders was used to record the mass variation using a load cell (FS2030-000X-0500-G, TE Connectivity, Schaffhausen, Switzterland) and also to obtain the variations of temperature on its slab surface using the thermographic camera Optris PI® 160 (Optris GmbH, Berlin, Germany). The other cylinder was used to monitor the temperatures of the surface and the centre using K-type thermocouples, and to measure dielectric properties with a two-needle sensor inserted into the centre of the sample and connected to the Agilent 4294A Impedance Analyzer. In addition, the temperature of a certified emissivity surface (Optris GmbH, Berlin, Germany) was recorded both using a K-type thermocouple and the thermographic camera. The ambient temperature was also recorded using another K-type thermocouple. All thermocouples and the load cell were connected to an Agilent 34901A multiplexer in a data acquisition equipment Agilent 34972A (Agilent Technologies, Malaysia), see figure 1.

The experiment, explained above, was repeated eight times, to obtain significant critical freezing temperatures.

The freezing of the samples was carried out at -40 °C for 35 minutes in an air forced freezing chamber (Model ACR-45/87, Dycometal, S.L, Barcelona, Spain). The samples were placed in the centre of the freezer, under turbulent conditions, on a support printed in PLA with a 3D printer. An extruded polystyrene insulation sheet (68 cm × 52 cm × 4 cm) was used as the freezer cover (Chovafoam type 4I, Leroy Merlin S.L., Valencia, Spain) with a hole in the middle for the thermographic camera.

2.2. Physicochemical parameters

Before and after freezing, the mass of the sample was measured using a Mettler Toledo AB304-S precision balance (± 0.001) and water activity was measured with a Decagon Aqualab, series 3 TE dew point hygrometer (± 0.003) (Decagon Devices Inc., USA). The moisture of the fresh product was obtained following the ISO 1442 (1997) standard for meat products, drying the samples at 105 °C and atmospheric pressure for 48 hours.

2.3. Infrared thermography

Thermal images were acquired using the Optris PI 160 Thermal Imager (Optris GmbH, Berlin, Germany). It uses a two-dimensional focal plane array with 160x120 pixels, a spectral range of 7.5 to 13 µm, a resolution of 0.05 °C, and an accuracy of ± 2%. The camera measures a temperature range between -20 and 900 °C. It has a field of view of 23°x17° with a minimum distance of 2 cm. The camera uses Optris PI Connect software (Optris GmbH, Berlin, Germany). The camera was directly connected to a computer to record the entire process. A certified emissivity surface of 25 mm diameter ($\varepsilon = 0.95$) (Optris GmbH, Berlin, Germany) was used as reference to calculate the reflected energy received by the infrared camera.

2.4. Dielectric properties

The sensor consists of two steel-needles with 10 mm long, 0.8 mm of diameter and 1.3 mm of distance between needles. The sensor was inserted into the centre of the sample, penetrating from the lateral surface of the cylinder (through the cylindrical surface), so that the dielectric properties were measured perpendicular to the direction of the fibres (figure 6). The sensor was developed in The institute of Food Engineering for Development (IuIAD), at the Politechnic University of Valencia (Traffano-Schiffo, 2021). The sensor was connected to a 4294A impedance analyzer (Agilent Technologies, Santa Clara, CA, USA). Permittivity was estimated using equations (1-3) (see Results Sections). Dielectric spectrum was measured in the frequency range from 40 Hz to 1 MHz. The equipment calibration was performed in open (air) and short-circuit.

2.5. Differential scanning calorimetry (DSC)

T_g' and the mass fraction of freezable water values was determined using a Differential Scanning Calorimeter (DSC, 1 StareE System, Mettler-Toledo, Switzerland). Poultry meat samples (10 to 20 mg) were accurately weighted using Mettler Toledo XS-205 balance into 40 µL DSC aluminum pans (Mettler

Toledo, ME-00026763). Filled pans were hermetically sealed. An empty aluminium pan was used as a reference in all measurements. Liquid nitrogen was used as coolant, poured into the cooling can of the DSC equipment; gas nitrogen was flowed in the purge line, to control the environment of the sample, with a flow rate of 60 mL/min. Calibration was performed by FlexCal, an automatic calibration function supplied by the manufacturers. To perform the experiments, the samples were cooled at 5 °C/min until -80 °C, held for 15 min, warmed to the annealing temperature (-20ºC, based on the work of Delgado and Sun, 2002), held for 60 min, cooled at 5 °C/min until -80 °C, held for 15 min and scanned at 5 °C/min until 20 °C. The protocol followed in this research work was the one established by Delgado and Sun (2002). These authors improved the protocol of Brake and Fennema (1999) which was based on the method used by Carrington et al. (1994) involving annealing. The glass transition analysis reports the starting, midpoint and end temperatures of a step, once the limits of the transition was provided, and the midpoint temperature was taken as T_g'. Mass fraction of freezeable and unfreezeable water was estimated by the proposed method of Ross (1978), described in Delgado and Sun (2002).

DSC measurements were made by triplicate. The obtained data was analyzed with the DSC software provided (STARe software, Mettler Toledo, Barcelona, Spain).

3. Results and discussion

In this experiment, the chicken breast has been selected since in the industrial freezing processes by IQF (Individual Quick Freezing) chicken is frozen butched, being the parts most used in freezing the breast, thighs and wings.

The freezing of the chicken breast samples was carried out in an air forced freezing chamber at −40 °C. An example of temperature evolution of the centre of the sample throughout the process can be observed in Figure 2. In the figure it can be observed that the temperature falls below zero degrees, and the onset of freezing occurs at temperatures close to -1.6 °C, reaching freezing temperatures of -4 °C due to the cryoscopic decrease. The duration of the freezing process is approximately 7 minutes due to the small size of the sample. After this time there is a drop in temperature until the sample equilibrates at -40 °C, which is the freezing air temperature.

Glass transition temperature is important for food stability (Delgado and Sun, 2002). The glass transition temperature of the maximum cryo-concentrated solution (Tg') was measured in annealed samples by using Differential Scaning Calorimetry. Figure 3 shows an example of the thermogram obtained. In the figure, the glass transition is clearly appreciated. An average of Tg' value of -16.73 ± 0.13 °C was obtained. This value is close to that obtained by other authors for chicken meat: -17.08 °C (Akköse, 2018); -16.83 °C (Delgado and Sun, 2002); -16.63 (Sunooj et al., 2009). The unfreezeable water content has been also estimated by DSC, 0,23 ± 0,02 kg_w/kg_T similar than the value obtained by Delgado and Sun (2002).

Different analysis techniques based on photonics in the radio frequency range to analyze the freezing process were used by research groups from different fields; it is possible to classify these analyzes into two groups: first the impedance analysis, focusing on the reactance, and the second the analysis of the dielectric properties, focusing on the permittivity.

In a study published by Chin et al., (2007) it is explained that the appearance of an ice phase in a dielectric medium produces a phenomenon in the radiofrequency impedance spectrum, which allows detecting the onset of freezing. Smith and Polygalov (2019), determine a procedure for the detection of the initiation of nucleation by analyzing the imaginary part of the impedance, the reactance. Figure 4 shows the reactance spectra in the radio frequency range of a of chicken breast sample during freezing. Figure 4a shows the reactance spectra of the first process times (meat refrigeration from 0 to 370 s), following with the typical gaussian bell shape in the early stages of freezing (660 s) and finishing with the reactance spectra in the glass transition (840 s). The same spectra at long freezing times are shown in Figure 4b. It is possible to observe how the frequencies at which the maximum reactance appear are of the order of MHz and at the end of the freeze the order is of kHz.

Figure 5 shows the exponential relationship of the maximum effect on reactance and the corresponding relaxation frequency of this phenomenon, compared to the temperature of the sample. As can be seen in this figure, it has not been possible to determine the onset of the phenomenon, since the initial relaxation frequencies are greater than the measurement range of the equipment used (1 MHz). Therefore, this technique requires a measurement equipment capable of analyzing freezing at frequencies close to the microwave spectrum. Furthermore, the representation of the maximum reactance values and their respective frequencies do not allow to determine any change in the physical properties of the meat during the freezing process. For this reason, this technique is not useful to determine quality properties during the meat freezing process, in which the properties of the tissue are as important at the beginning of freezing as at any other key point of freezing process, such as point of maximum cryoconcentrated liquid phase or the glass transition.

As the emitter and the receiver are arranged in parallel, the impedance measurements have been transformed into dielectric properties according to the equations 1, 2 and 3 (figure 6). Considering that its capacitance in vacuum is a function of the geometry of the sensor and its value is equal to 0.175 pF (equation 1 in figure 6).

Figure 7 shows an example of the evolution of the spectra of complex permittivity, dielectric constant (ε') and loss factor (ε'') at different freezing times, where it is possible to observe how the spectra decrease in value as the freezing process progresses.

In order to describe the effect of tissue on photons, it is necessary to obtain the alpha and beta relaxations properties in the radiofrequency range. For this purpose, the Traffano-Schiffo model (eq. 4) was applied (Traffano-Schiffo et al., 2017):

$$l\varepsilon'(\omega) = l\varepsilon'_{\infty} + \sum_{n=1}^{3} \frac{\Delta l\varepsilon'_n}{1+e^{((l\omega^2 - l\varpi_\tau{}^2)*\alpha_n)}} \quad (4)$$

Where, $l\varepsilon'$ represents the decimal logarithm of the dielectric constant, $l\varepsilon'_{\infty}$ the logarithm of the dielectric constant at high frequencies, lω represents the decimal logarithm of the angular frequency, $\Delta l\varepsilon'_n$ ($\Delta l\varepsilon'_n = \log\varepsilon'_n - \log\varepsilon'_{n-1}$) the amplitude of the dispersion, $l\omega_t$ the logarithm of the angular frequency at relaxation time for each dispersion n, and α_n are the dispersion slopes. Following Traffano-Schiffo et al., 2017, it is possible to estimate the dielectric constant at relaxation frequencies, (ε'_α and ε'_β) and the relaxation frequencies (f_α and f_β).

Some authors describe the possibility of determining first or second order transitions in protein structures from the permittivity in the radiofrequency spectrum. In this sense, Roos (2010) explains that it is possible to determine the glass transition of proteins or even freezing processes in the variation of the loss factor in the beta relaxation. In this sense, the beta dispersion represents the orientation and induction of the fixed charges of the macromolecules, or the surface charges associated with surface tension phenomena, also called the Maxwell-Wagner phenomenon. For this reason, the appearance of ice Ih, with a hexagonal crystal conformation, with a high surface tension, which allows it to quickly attract the closest molecules of liquid water, can generate an interaction in the beta dispersion, which should change according to the variation of surface tension throughout the freezing process.

Figure 8 shows, in black, the evolution of the dielectric constant and, in gray, the evolution of the loss factor, in the beta dispersion during the freezing process. In both, a minimal change is observed until the beginning of freezing is reached, at -1.32 °C ± 0.7 °C, which can be considered as the initial freezing temperature. This agrees with the measurements observed in the freezing curve (Figure 2), around -1.6 °C. Both curves reach a maximum value at a temperature of -3.4 °C ± 1.2 °C, which could represent the end point of freezing, which in the case of the freezing curve was estimated to be around -4 °C.

According to Roos (2017), the glass transition can be determined in the decrease of the loss factor, at the point of the change of slope. In figure 8 it is possible to determine this point at -17.50 ± 1.05. However, it is difficult to correctly determine this point because in beta dispersion, the loss factor is influenced by the Maxwell-Wagner phenomenon and by ionic conductivity, being the meat a strongly ionic system. An alternative is the use of the dielectric constant, which is only influenced by the Maxwell-Wagner phenomenon. In figure 8 it is possible to see how the dielectric constant becomes constant with respect to the temperature upon reaching the glass transition. Therefore, the dielectric constant in the beta dispersion is more reliable for the determination of the glass transition than the loss factor.

The alpha dispersion represents the interactions of low weight ionic molecules, such as electrolytes, with a flux of photons in the radio frequency spectrum. The electrolytes in the meat liquid phase will have interactions with the ice, so it is possible to think that the value of the permittivity in this dispersion will change as ice is formed.

Figure 9 shows the variation of the dielectric constant in the alpha dispersion throughout freezing. It is possible to observe, as the beta dispersion analysis showed, that the value of the dielectric constant remains almost constant until reaching a value, which, in this case, corresponds to a temperature of -2.17 ± 0.91 and rises to a maximum which corresponds to a temperature of -4.9 ± 1.6. The critical temperatures observed in the alpha dispersion are lower than in the beta dispersion, this difference may be due to the fact that the beta dispersion is a direct measure of the interaction of ice with the photons field, while the alpha measure is an indirect measure of the state of the ice, since it analyzes the state of the electrolytes. It means, that the spin orientation of electrolytes is changing with the variation of ice surface tension. Alpha dispersion detects this electrolytic phenomenon and, indirectly, the ice surface variation with delay. For this reason, the measurements in alpha dispersion suffer a delay of the phenomenon, in terms of freezing temperature.

For these reasons, it is possible to conclude that the measurement of the dielectric constant in the beta dispersion makes it possible to determine the critical temperatures of the food freezing process, initial freezing temperature (Tm_0), the freezing temperature of sample with the maximally freeze-concentrated solute matrix (Tm') or the glass transition temperature of the maximally freeze-concentrated solute matrix (Tg').

4. Conclusions

The critical temperatures of the food freezing process, initial freezing temperature, the freezing temperature of sample with the maximally freeze-concentrated solute matrix or the glass transition temperature of the maximally freeze-concentrated solute matrix of chicken breast have been determined by means of calorimetry techniques, being similar than those of other authors. Moreover, these temperatures were determined using photospectrometry in radiofrequency range, showing that this technique is fast, reliable, and easy to implement in a dynamic freezing system.

5. Declaration of competing interest

There are no conflicts to declare.

6. Acknowledgements

This paper is part of the I+D+i PID2020-116816RB-I00 project, funded by MCIN/ AEI/10.13039/501100011033.

7. References

Akköse, A., 2018. Effect of Various Biopolymers on Glass Transition Temperature of Chicken Breast Meat. Akademik Gıda 16, 120–126. https://doi.org/10.24323/akademik-gida.449572

Baker-Jarvis, J.; Kim, S. The Interaction of Radio-Frequency Fields with Dielectric Materials at Macroscopic to Mesoscopic Scales. J. Res. Natl. Inst. Stand. Technol. 2012, 117, 1–60.

Brake, N.C., Fennema, O.R., 1999. Glass transition values of frozen muscle tissue. J. Food Sci. 64 (1), 10–15.

Carrington, A.K., Sahagian, M.E., Goff, H.D., Stanley, D.W., 1994. Ice crystallization temperatures of sugar/polysaccharide solutions and their relationship to thermal events during warming. Cryo Letters 15 (4), 235–244.

Castro-Giráldez, M., Balaguer, N., Hinarejos, E., Fito, P.J., 2014. Thermodynamic approach of meat freezing process. Innovative Food Science & Emerging Technologies 23, 138–145. https://doi.org/10.1016/j.ifset.2014.03.007

Chen, C.S., 1986. Effective Molecular Weight of aAqueous solutions and liquid foods calculated from the freezing point depression. Journal of Food Science, 51(6), 1537-1539

Chin, K.B., Buehler, M.G., Seshadri, S., Keymeulen, D., Anderson, R.C., Dutz, S., Narayanan, S.R., 2007. Investigation of water and ice by ac impedance using electrochemical properties cup. Review of Scientific Instruments 78, 016104. https://doi.org/10.1063/1.2424443

Chirife, J., Fontan, C.F., 1980. Prediction of water activity of aqueous solutions in connection with intermediate moisture foods: experimental investigation of the aw lowering behavior of sodium lactate and some related compounds. Journal of Food Science 45, 802–804. https://doi.org/10.1111/j.1365-2621.1980.tb07453.x

Delgado, A.E., Sun, D.-W., 2002. Desorption isotherms and glass transition temperature for chicken meat. Journal of food engineering 55, 1–8.

Elliot, G.D., Wang, S., Fuller, Barry, J., 2017. Cryoprotectants: A review of the actions and applications of cryoprotective solutes that modulate cell recovery from ultra-low temperatures. Cryobiology 76, 74-91. http://dx.doi.org/10.1016/j.cryobiol.2017.04.004

Gordon, M., Taylor, J.S. 1952. Ideal copolymers and the second-order transitions of synthetic rubbers. i. non-crystalline copolymers. Journal of Chemical Technology and Biotechnology, 2(9), 493-500. https://doi.org/10.1002/jctb.5010020901

Hellmuth, O., Schmelzer, J.W.P., Feistel, R., 2020. Ice-Crystal Nucleation in Water: Thermodynamic Driving Force and Surface Tension. Part I: Theoretical Foundation. Entropy 22, 50. https://doi.org/10.3390/e22010050

Horie, K.; Ushiki, H.;Winnik, F.M. Molecular Photonics; Wiley: New York, NY, USA, 2000.

Kumar, P.K., Rasco, B.A., Tang, J., Sablani, S.S., 2020. State/Phase Transitions, Ice Recrystallization, and Quality Changes in Frozen Foods Subjected to Temperature Fluctuations. Food Eng Rev 12, 421–451. https://doi.org/10.1007/s12393-020-09255-8

Mahanta, A.K., Rana, D., Sen, A.K., Maiti P., 2017. Thermal Properties of Food and Biopolymer Using Relaxation Techniques. In Ed: Roos, Y.H., Ahmed, J. Glass Transition and Phase Transitions in Food and Biological Materials. JohnWiley & Sons Ltd. Oxford (UK). 141-158

Robinson, R.A., Stokes, R.H., 2002. Electrolyte solutions. Courier Corporation.

Roos, Y.H., 2021. Glass Transition and Re-Crystallization Phenomena of Frozen Materials and Their Effect on Frozen Food Quality. Foods 10, 447. https://doi.org/10.3390/foods10020447

Roos, Y.H., 2010. Glass transition temperature and its relevance in food processing. Annual review of food science and technology 1, 469–496. https://doi.org/10.1146/annurev.food.102308.124139

Ross, K.D., 1978. Differential scanning calorimetry of nonfreezable water in solute—macromolecule—water systems. Journal of Food Science 43, 1812–1815.

Roudaut, G., Simatos, D., Champion, D., Contreras-Lopez, E., Le Meste, M., 2004. Molecular mobility around the glass transition temperature: a mini review. Innovative Food Science & Emerging Technologies 5, 127–134. https://doi.org/10.1016/j.ifset.2003.12.003

Roychoudhuri, C.; Kracklauer, A.F.; Creath, K. The Nature of Light: What Is a Photon; CRC Press: New York, NY, USA, 2008.

Smith, G., Polygalov, E., 2019. Through Vial Impedance Spectroscopy (TVIS): A Novel Approach to Process Understanding for Freeze-Drying Cycle Development, in: Ward, K.R., Matejtschuk, P. (Eds.), Lyophilization of Pharmaceuticals and Biologicals: New Technologies and Approaches, Methods in Pharmacology and Toxicology. Springer, New York, NY, pp. 241–290. https://doi.org/10.1007/978-1-4939-8928-7_11

Sunooj, K.V., Radhakrishna, K., George, J., Bawa, A.S., 2009. Factors influencing the calorimetric determination of glass transition temperature in foods: A case study using chicken and mutton. Journal of Food Engineering 91, 347–352. https://doi.org/10.1016/j.jfoodeng.2008.09.014

Traffano-Schiffo, M.V., Castro-Giráldez, M., Colom, R.J., Fito, P.J., 2017. Development of a Spectrophotometric System to Detect White Striping Physiopathy in Whole Chicken Carcasses. Sensors 17, 1024. https://doi.org/10.3390/s17051024

Traffano-Schiffo, M.V., Castro-Giráldez, M., Colom, R.J., Talens, P., Fito, P.J., 2021. New methodology to analyze the dielectric properties in radiofrequency and microwave ranges in chicken meat during postmortem time. Journal of Food Engineering 292, 110350. https://doi.org/10.1016/j.jfoodeng.2020.110350

Traffano-Schiffo, M.V., Castro-Giráldez, M., Herrero, V., Colom, R.J., Fito, P.J., 2018. Development of a non-destructive detection system of Deep Pectoral Myopathy in poultry by dielectric spectroscopy. Journal of Food Engineering 237, 137–145. https://doi.org/10.1016/j.jfoodeng.2018.05.023

van der Sman, R.G.M., 2020. Impact of Processing Factors on Quality of Frozen Vegetables and Fruits. Food Eng Rev 12, 399–420. https://doi.org/10.1007/s12393-020-09216-1 van der Sman, R.G.M., Boer, E., 2005. Predicting the initial freezing point and water activity of meat products from composition data. Journal of Food Engineering 66, 469–475. https://doi.org/10.1016/j.jfoodeng.2004.04.018

You, Y., Kang, T., Jun, S., 2021. Control of Ice Nucleation for Subzero Food Preservation. Food Eng Rev 13, 15–35. https://doi.org/10.1007/s12393-020-09211-6

FIGURES

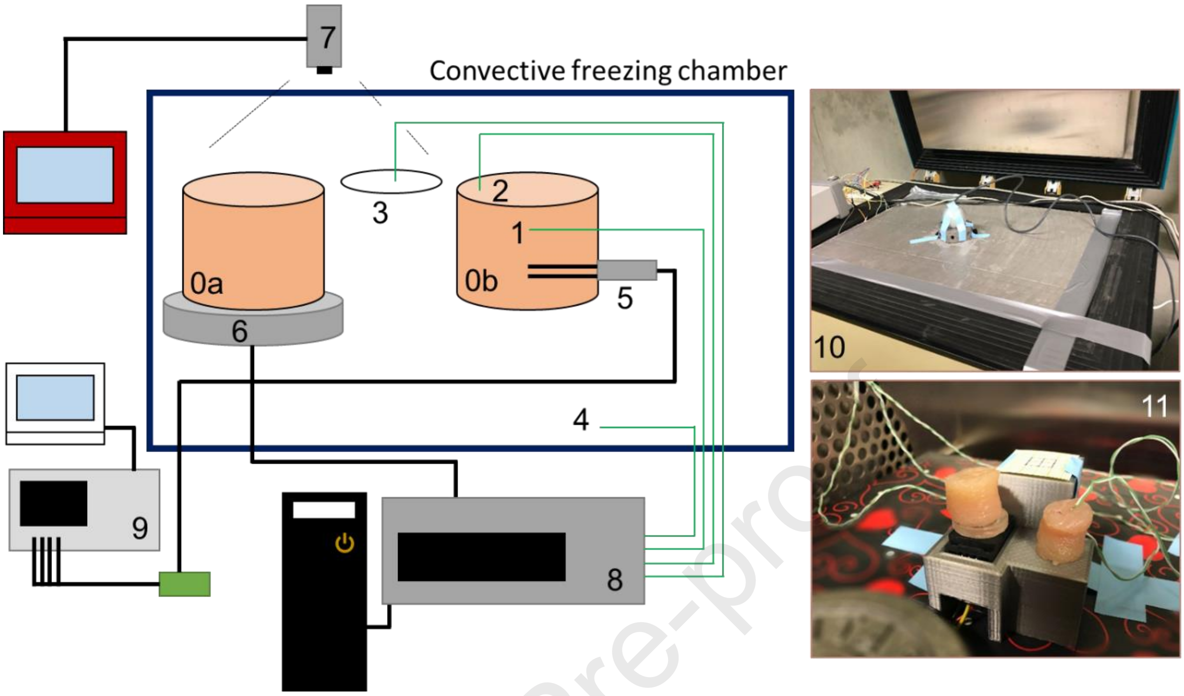

Figure 1. Experimental setup diagram. 0a, Sample to measure weight and surface temperature by FTIR; 0b, Sample to measure dielectric properties and temperatures using the thermographic camera and K-type thermocouples; 1, K-type thermocouple to measure the temperature of the sample centre; 2, K-type thermocouple to measure the temperature of the sample surface; 3, Certified emissivity surface and K-type thermocouple to measure its temperature; 4 K-type thermocouple to measure the air temperature; 5, Two-needle dielectric sensor; 6, Load cell; 7, Infrared Camera; 8, Data acquisition equipment Agilent 34972A; 9, Agilent 4294A Impedance Analyzer; 10, picture of the extruded polystyrene insulation sheet, with a hole for the thermographic camera, used as the freezer cover; 11, picture of the internal assembly.

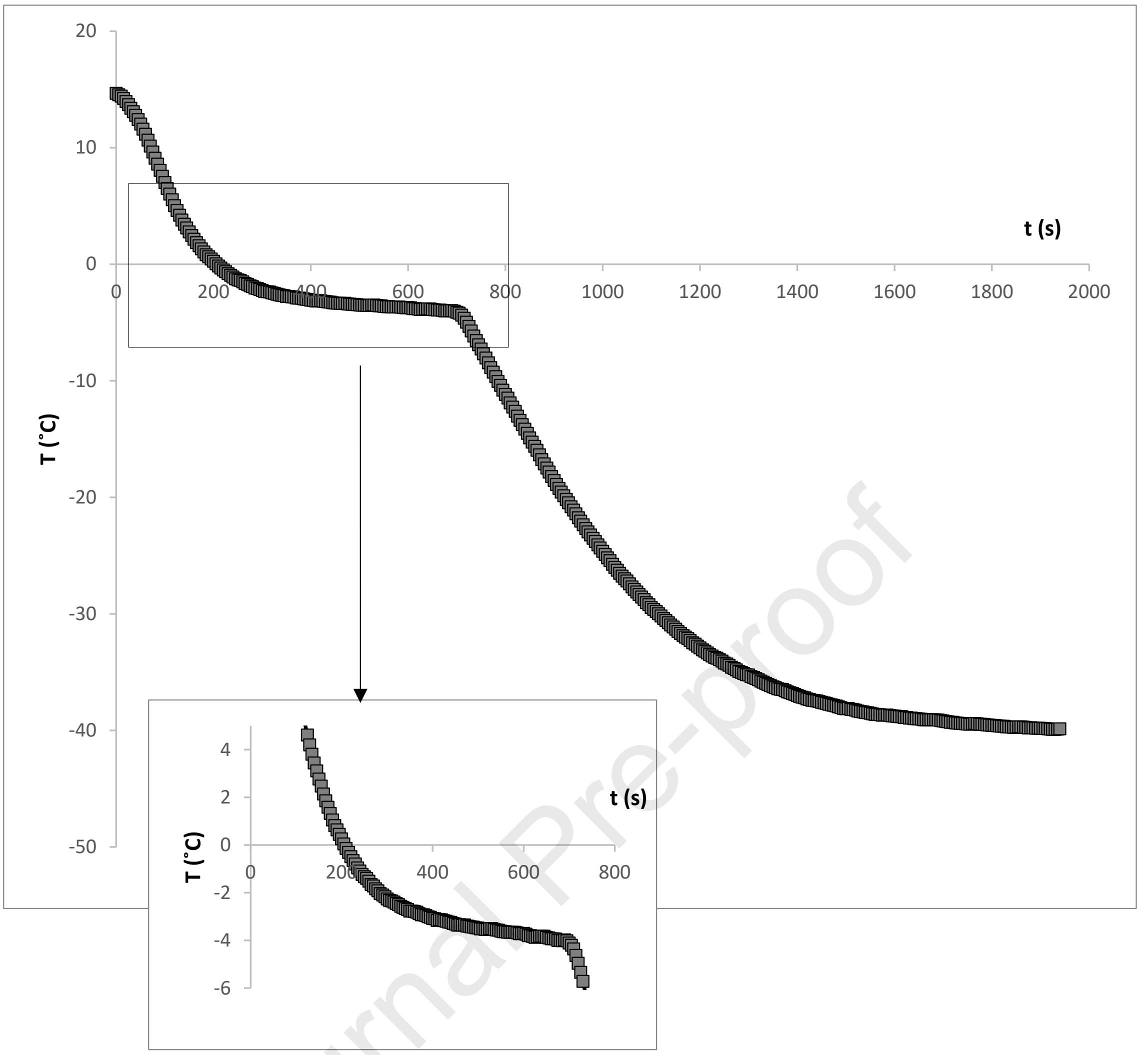

Figure 2. Freezing curve of one meat breast sample in an air forced freezing chamber at −40 °C.

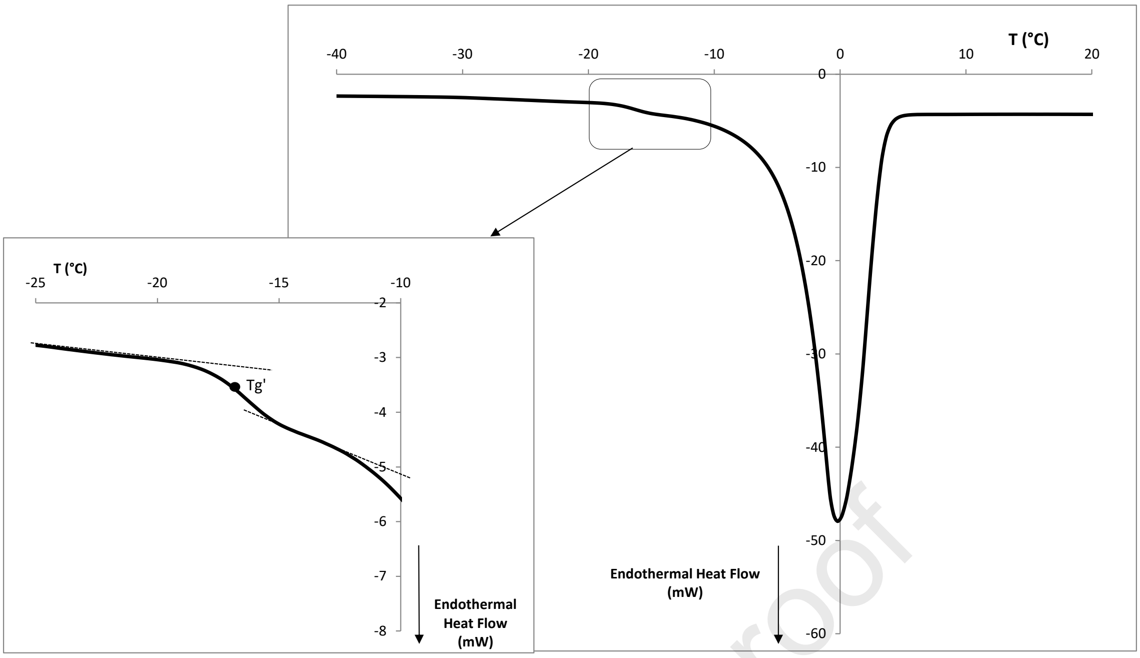

Figure 3. DSC thermogram for meat breast samples. A detailed of glass transition and the location of Tg' are also shown.

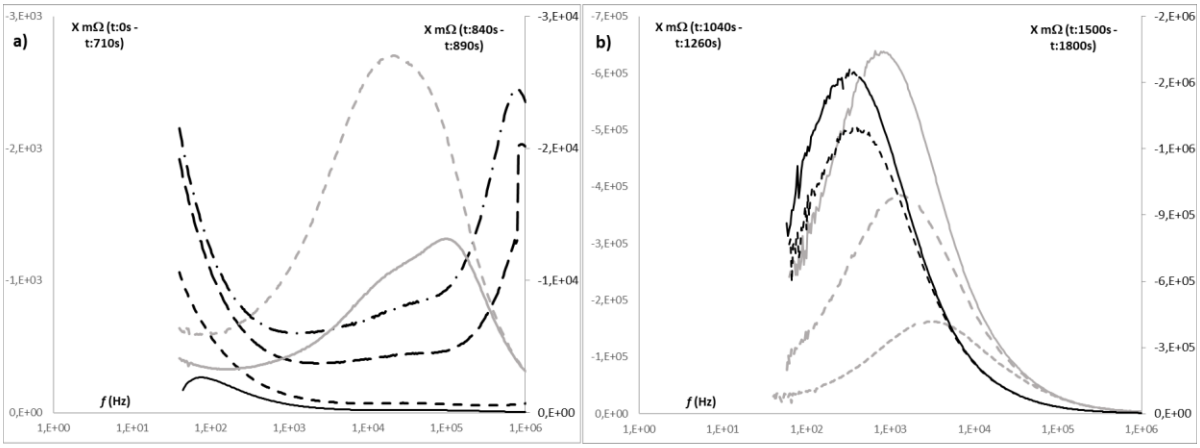

Figure 4. Reactance spectrum during the breast freezing process of one sample, where a) represents the freezing time from 0 to 890 s (on the left, — 0 s; --- 370 s; – – 660 s and – · – 710 s, and on the right, — 840 s and -- 890 s) and b) from 1040 to 1800s (on the left -- 1040 s; – – 1140 s and — 1260 s, and on the right -- 1500 s and — 1800 s).

359 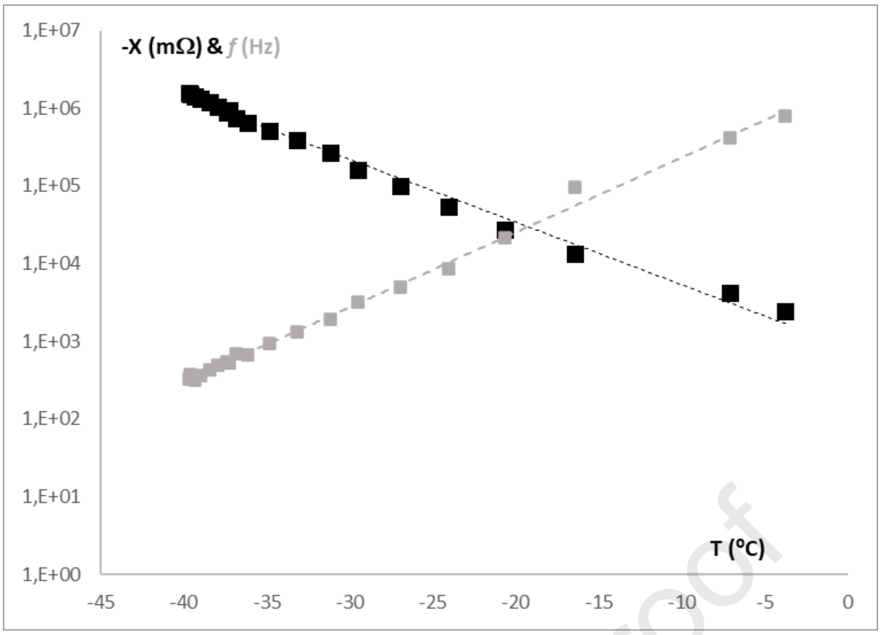

360 **Figure 5.** Relaxation reactance (■) and frequency (■) versus temperature in one sample freezing process.

361

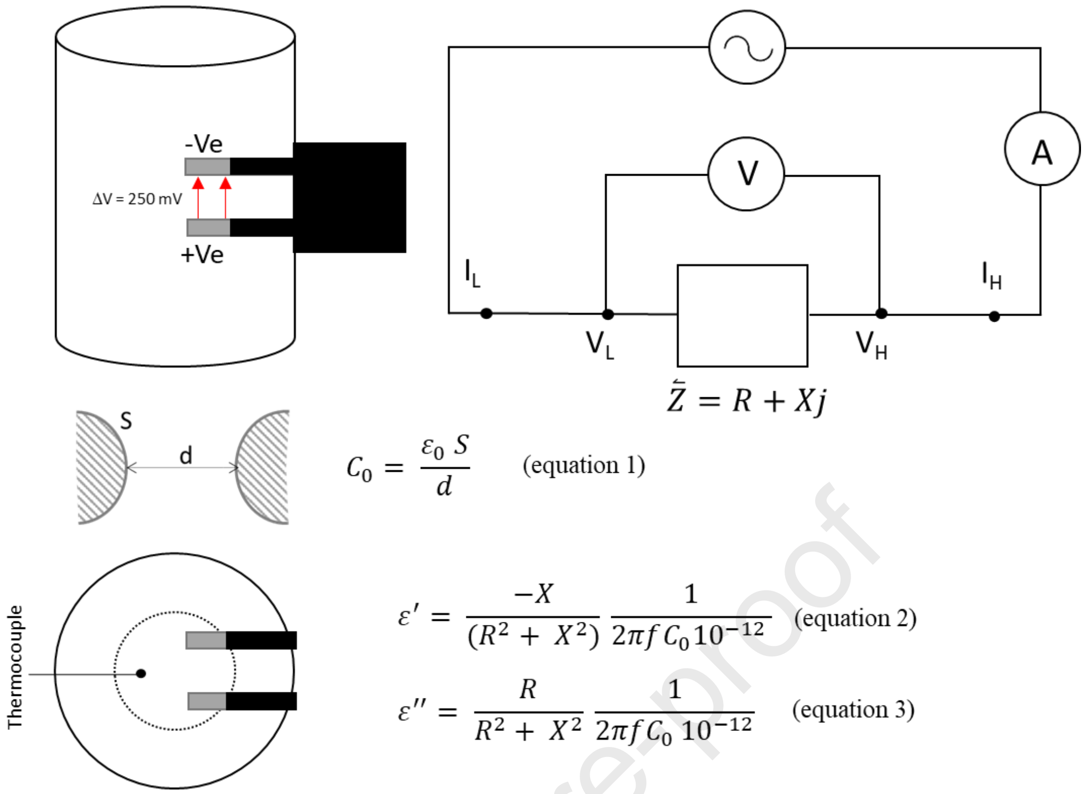

Figure 6. Diagram of sensor based on impedance measurements, the electric circuit, the detail of capacitance in vacuum determination and the equations used to determine the complex permittivity.

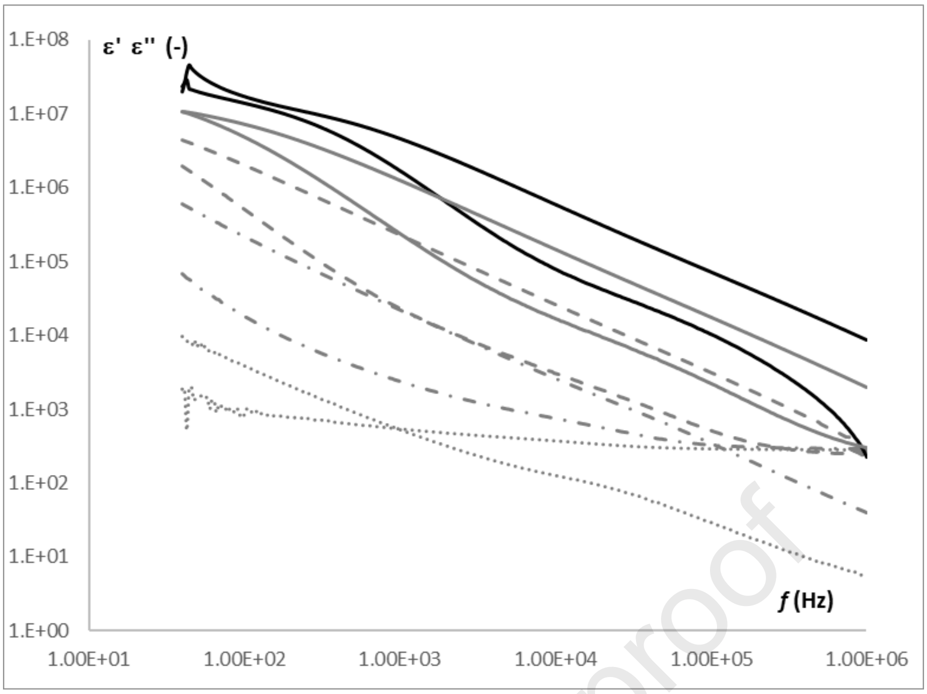

Figure 7. Permittivity spectra of one freezing process sample, were — is 0s; — is 370 s; – – is 660 s; – · – is 840 s and ···· is 1410 s.

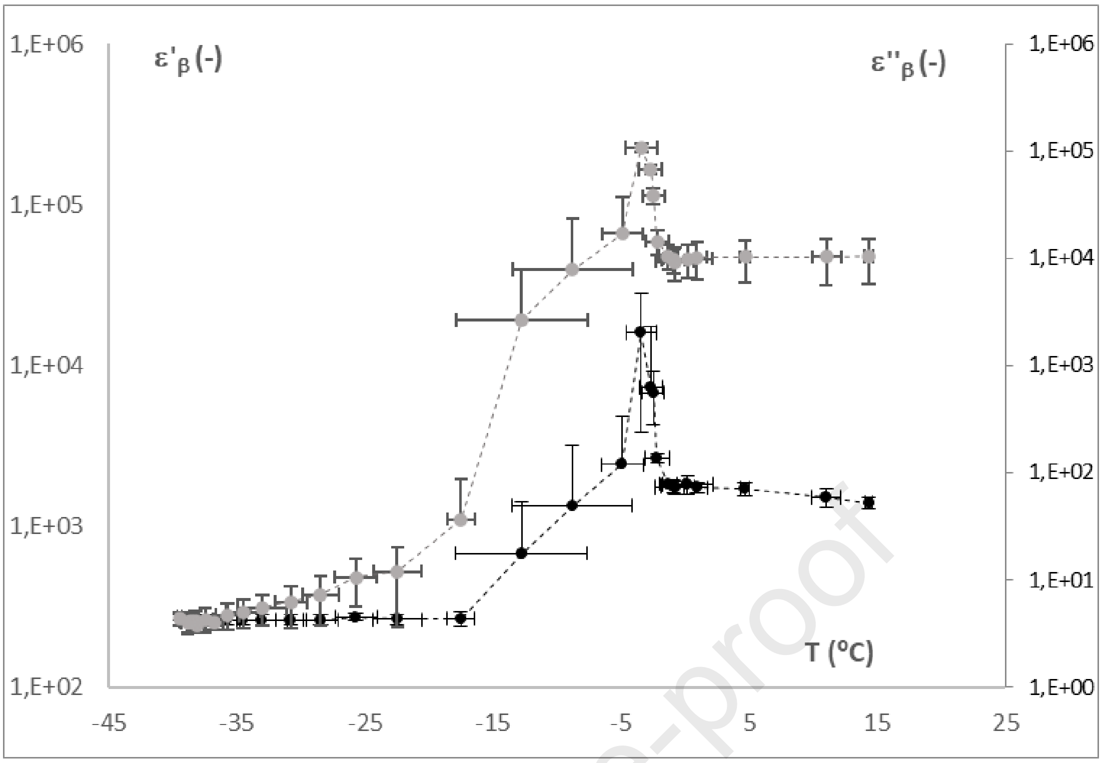

Figure 8. On the left dielectric constant (●) and on the right loss factor (●) in beta relaxation versus temperature.

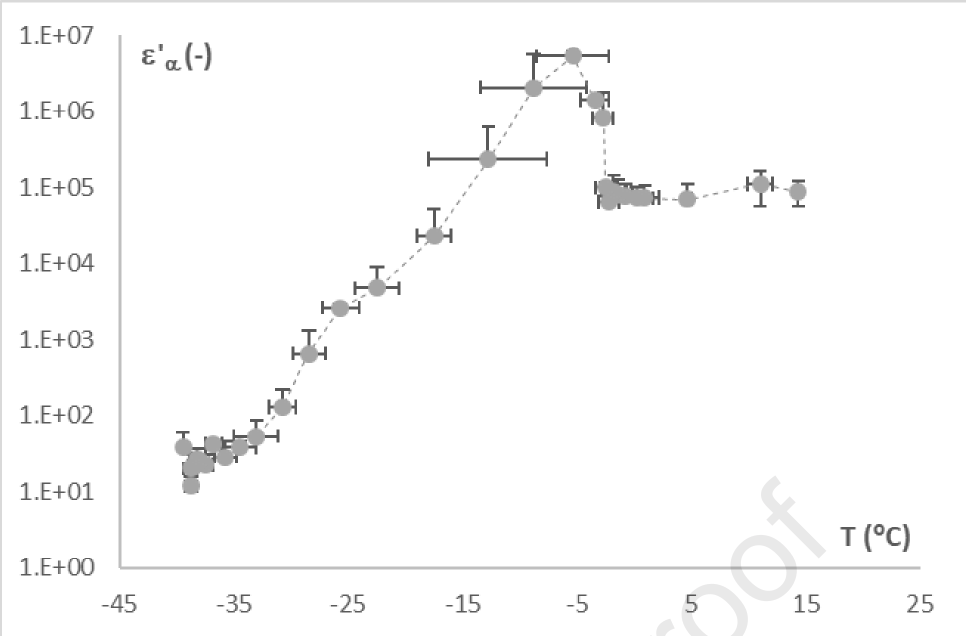

Figure 9. Dielectric constant in alpha relaxation versus temperature.

RESEARCH HIGHLIGHTS

> Permittivity in β dispersion is useful to determine key freezing temperatures.

> Photospectrometry in RF demonstrated its reliability and accuracy for this purpose.

> Photospectrometry was compared with calorimetric techniques with good results.

Declaration of interests

☒ The authors declare that they have no known competing financial interests or personal relationships that could have appeared to influence the work reported in this paper.

☐ The authors declare the following financial interests/personal relationships which may be considered as potential competing interests: